Experimental determination of rolling element bearing stiffness

Experimental Determination of Rolling Element Bearing Stiffness

A. de Kraker*, R.J.W. Knaapen, L. Kodde, D.H. van Campen
Department of Mechanical Engineering, Eindhoven University of Technology
5600 MB Eindhoven, The Netherlands
Email: kraker@wfw.wtb.tue.nl

Abstract
In 1990, Lim and Singh presented a complete 6-dof roller-bearing stiffness model. The experimental verification (using an instrumental variables identification procedure) of all the stiffness coefficients of such a bearing appeared to be difficult, because the experimental setup showed some unexpected properties. In this paper the (modified) experimental setup will be presented to get reproducible measurements. Estimating all the stiffness matrix coefficients simultaneously from measured transfer functions still appeared to be unfeasible. Therefore, a 1-dof amplitude fit procedure has been applied. The results appear to be very promising and applicable in practice, but future research certainly is necessary to understand the remaining differences between the mathematical model and measurements. In addition to stiffnesses, the procedure also gives damping values. Finally, matters such as hysteresis, reproducibility and reciprocity have been investigated.

1. Introduction

Noise and vibration generated by rotating mechanical equipment have always been a problem in the implementation of new technology in automobiles, rotorcrafts and industrial machines. In many rotating systems, the vibration transmission through roller-bearings is very important. Hence, for a reliable mathematical model of the overall dynamic system, a thorough understanding of the vibration transmission mechanism through bearings, and the role of bearings as a dynamic coupler between the shaft and casing, is essential. In general, existing bearing models only describe radial and axial stiffnesses. Many experiments however have shown the importance of flexural or out-of-plane type deformations. In 1990, Lim and Singh have presented a 6-dof bearing stiffness model (3 transl./3 rot.), see [1], and this model is further improved by Van Roosmalen in 1994 by taking a non-uniform load distribution on the line contact between the inner race, roller and outer race of the bearing (see [3], [4]).

A first experimental approach to identify the complete bearing stiffness matrix with an instrumental variables identification algorithm [2] did not lead to sufficiently accurate results due to non-reproducibility of the measurements and inaccuracy in the torque stiffnesses. Applying higher preloads was thought to be the best solution to this problem, as in practice no rolling element is allowed to lose contact.

In this paper an updated experimental setup is presented by which bearing stiffnesses can be measured, without the occurrence of non-reproducibility and with high accuracy in the rotational stiffnesses. Subsequently, the experimentally determined stiffness can be compared to the theoretical

*Address all correspondence to this author.

model which gives a decisive answer to the question whether the model is suitable for the accurate prediction of rolling element bearing stiffnesses, used for vibration prediction purposes.

2. The Bearing Model

In the extended bearing model mentioned before, 3 translational and 3 rotational dof's are taken into account, leading to a 6×6 stiffness matrix. The model can be used for deep groove ball bearings, angular contact ball bearings, straight roller bearings and taper roller bearings under the following assumptions.

2.1 Assumptions

- Elliptical contacts for ball-bearings and rectangular contacts for roller bearings.
- Contact angles of the ball types may change, but for the roller types they are assumed to be constant.
- Each bearing is characterized by its kinematic and design parameters, such as: unloaded contact angle α_0, radial clearance r_L, effective stiffness coefficient K_n for each ring-rolling element-ring contact, preloads, inner raceway groove curvature radius for ball type and bearing pitch radius for roller type.
- Mean bearing displacements as shown in Figure 1 are given by the relative rigid body motions between the inner and outer rings.
- Hertzian contact stress theory is valid.
- Relative rolling element position is fixed.
- No centrifugal forces or gyroscopic effects.
- No tribological effects.
- Zero-stiffness axial rotation.

2.2 Load-displacement functions

For the derivation of the relations between the bearing forces and moments [F_{xbm}, F_{ybm}, F_{zbm}, M_{xbm}, M_{ybm}] and the global bearing displacements [q_{bm}] as given in Figure 1 we refer to the paper of Lim [1].

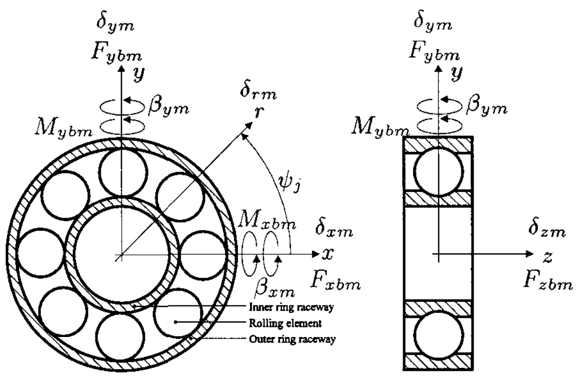

Figure 1: Rolling element bearing kinematics and coordinate system

A symmetric bearing stiffness matrix of dimension 6×6 can be defined for: $w, i = x, y, z$ as:

$$K_{bm} = \begin{bmatrix} \frac{\partial F_{wbm}}{\partial \delta_{im}} & \frac{\partial F_{wbm}}{\partial \beta_{im}} \\ \\ \frac{\partial M_{wbm}}{\partial \delta_{im}} & \frac{\partial M_{wbm}}{\partial \beta_{im}} \end{bmatrix}_{[q_{bm}]} \quad (1)$$

Each stiffness coefficient is evaluated at the static equilibrium point [q_{bm}]. It can be proved that the matrix is symmetric. For explicit expressions we refer to [1] and numerical values can be generated by the programme 'Lager', see [4].

2.3 Model characteristics

To get an impression of this bearing model, some characteristics of the model will be presented. For 2 bearing-types, a normal NSK 6208 deep groove ball bearing and a fictitious angular contact NSK 6208 bearing (contact angle of $\alpha_0 = 40^o$) some typical results are shown in Figure 2. The figure gives the stiffness matrix for an *increasing* radial preload in y-direction combined with a *constant* axial preload of 800 [N]. The simulations also show that sometimes small preload variations lead to large stiffness matrix component variation. Therefore the excitations must be accurately aimed in the right direction.

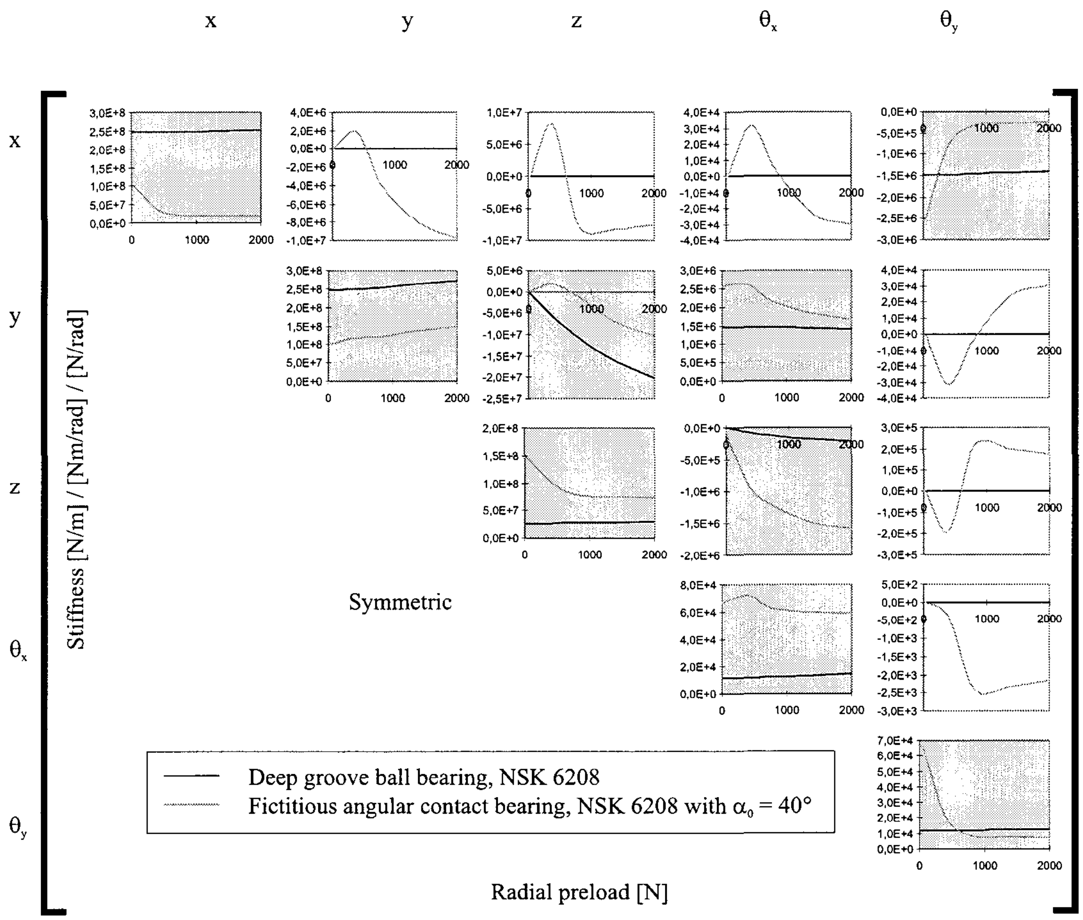

Figure 2: The stiffness matrix K_{bm} in case of an increasing radial preload in y-direction combined with a constant axial preload of 800 [N]

3. The Experimental Setup

The first experimental setup was combined with a Least Squares and Instrumental Variables method to identify all bearing stiffness coefficients simultaneously from measured transfer functions, see [2]. The results were unsufficiently convincing, mainly due to non-reproducibility of the data and still some non-understood differences between theory en practice. Whether this is due to model imperfections or unknown experimental shortcomings has not yet been found out. In this section an adapted experimental setup and identification procedure will be presented.

3.1 Potential Problems

In the mathematical model rollers can lose contact. In practice however, the presence of unloaded elements causes many problems. Sufficiently high preloads might be a solution to this problem. Secondly, the measurements are performed on a non-rotating shaft. Therefore, the measured transfer function could be dependent on the position of the rolling elements.

A bearing lubricant generates a significant damping effect, which might complicate the identification problem but has a positive effect on the problem of almost unloaded elements. When exciting the system, several eigenfrequencies show up not directly resulting from the bearing stiffness only. These effects have to be suppressed or should be incorporated in the model.

3.2 The Redesign

Several options have been investigated for the experimental setup, such as a (rigid) shaft and bearing in a very stiff support, a shaft and bearing in a flexible support (more realistic approach, both with non-rotating shaft) or a rigid rotor, with a fixed rotational speed rotating in 2 rigidly supported bearings as described by [6].
The first alternative has been chosen because of the simplicity of the model and the straightforward measurement procedure. In Figure 3 this setup is shown schematically. The preloads are applied by long strings and measured by strain gages and also checked by measuring the transversal violin-mode frequencies of the strings. The FRF-measurements are done by a PC-based, 4 channel signal analysis system (DIFA) with export to MATLAB for further data-analysis. The shaft is excited by a single or a pair of shakers, depending on the load situation. Both, the applied forces and the resulting accelerations are measured and passed to the DIFA system. During a measurement using transversal loading, the shaft will bend under the excitation load. When the bending stiffness has the same order of magnitude as the bearing stiffness, then not only this bending stiffness will have to be taken into account but also some effective mass has to be dealt with instead of the total mass of the shaft.

4. The Identification Process

In this section a brief outline will be given of the used identification algorithms. The Least Squares and Instrumental Variables Method were investigated and augmented with weighting factors in [2]. The third method, Amplitude Fitting [5], will be discussed and subsequently used for deriving new weighting factors, which will differ from the previous factors used in [2].

4.1 Identification Algorithms

Least Squares and Instrumental Variables identification algorithms are capable of performing multiple-degree-of-freedom (mdof) fits on mechanical systems like

$$\underline{M}\,\ddot{q} + \underline{B}\,\dot{q} + \underline{K}\,q = f \qquad (2)$$

The Least Squares algorithm minimizes the fit error by solving

$$[\underline{A}^T\underline{A}]\,\underline{\widehat{X}}_{ls} = \underline{A}^T\underline{E} \qquad (3)$$

in which $\underline{A}$ and $\underline{E}$ contain the model characteristics and the experimental data. $\underline{\widehat{X}}_{ls}$ contains the unknown parameters of Equation 2. The Instrumental Variables algorithm minimizes the difference between the measurements and the model by solving

$$[\underline{V}^T\underline{A}]\,\underline{\widehat{X}}_{iv} = \underline{V}^T\underline{E} \qquad (4)$$

iteratively. The matrix $\underline{V}$ contains the so-called instrumental variables output which can be considered as an estimate of the noise-free system.

4.2 Amplitude Fitting

Amplitude fitting [5] is appropriate if the amplitude of measured transfer functions is more accurate than the phase, and in essence it is a 1-dof fit procedure. A well separated peak in a transfer function can be approximated by a single mode response of

$$\ddot{y} + 2\,\Omega_k\,\xi_k\,\dot{y} + \Omega_k^2\,y = P_k\,e^{j\omega t} \qquad (5)$$

in which Ω_k and ξ_k are the structural frequency and damping for the particular mode k. P_k is the mode participation factor (reciprocal the modal mass). At a given frequency ω_i, the steady state amplitude of the response A_i is given by

$$A_i = \frac{P_k}{\sqrt{\left(\Omega_k^2 - \omega_i^2\right)^2 + \left(2\Omega_k\xi_k\omega_i\right)^2}} = \frac{P_k}{D_i} \qquad (6)$$

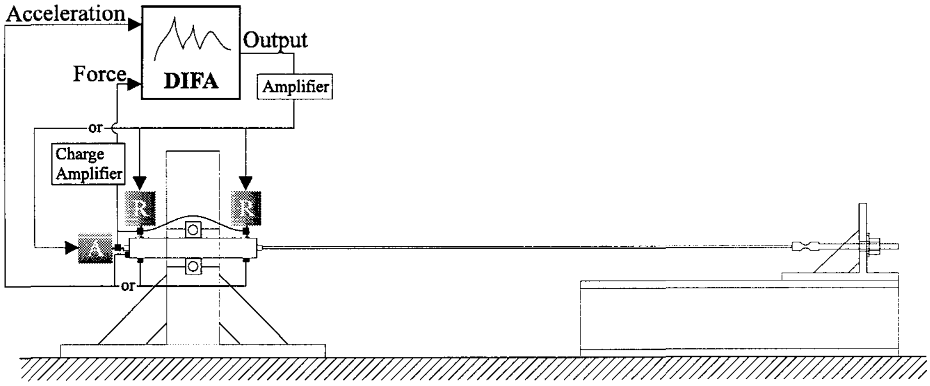

Figure 3: The measurement set-up, only axial pre-load mechanism is shown

which after amplitude scaling can be written as

$$A_i[A_iD_i - P_k] = 0 \tag{7}$$

Equation 6 will never be exact due to amplitude measurement errors, so we can write:

$$A_iD_i - P_k = -\varepsilon_iD_i \tag{8}$$

which indicates that the minimized error is $\sum_{i=1}^{n}(\varepsilon_iD_i)^2$, using least squares. Equation 7 with errors can be written as

$$(A_i + \varepsilon_i)^2\ D_i = (A_i + \varepsilon_i)\ P_k \tag{9}$$

or

$$\left(A_i^2 + 2\varepsilon_iA_i + \varepsilon_i^2\right) D_i = (A_i + \varepsilon_i)P_k \tag{10}$$

Simplifying Equation 10 using Equation 8 and neglecting the second order error terms, yields

$$A_i^2D_i - A_iP_k = -\varepsilon_iP_k \tag{11}$$

which shows that, when the problem is scaled, the minimized error is $\sum_{i=1}^{n}(\varepsilon_i)^2$, since P_k is a constant.

5. Experimental Results

It appeared not to be easy to estimate all the stiffness and damping terms for a bearing. This is probably caused by the fact that, in some FRF-components, coherences were too low for some frequency ranges. On the diagonal, the coherences are better. The results of a sdof fit procedure cannot be compared directly to matrix elements. Therefore, the results will be compared to the corresponding sdof fit on the theoretical transfer function as shown in Figure 4. For the actual sdof fits, the Instrumental Variables procedure is used.

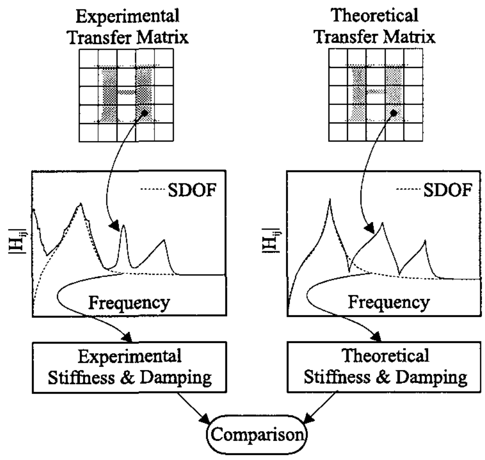

Figure 4: Comparision of experimental SDOF fit and theoretical SDOF fit

5.1 Stiffness and Damping Results

For a purely axial preload the radial stiffnesses in x and y-direction should be equal. This also applies to the rotational stiffnesses about the x and y-axis. Therefore, in theory, only three eigenfrequencies evolve. The **radial** stiffness and damping results for the

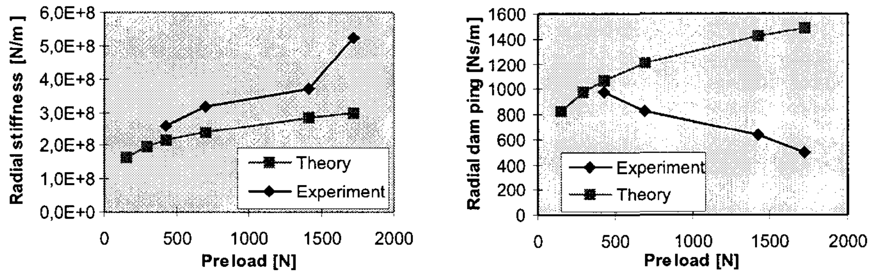

Figure 5: Left: The measured and theoretical *radial* stiffness. Right: The measured *radial* damping compared with the used Rayleigh damping. (Deep groove ball bearing NSK 6208)

deep groove ball bearing NSK 6802 are shown in Figure 5. The theoretical model shows the same trends as the experimental results but seems to need a multiplication to match with the experimental data, which could indicate an incorrect single roller element stiffness parameter. Using the sdof procedure, only the diagonal components can be studied directly. The so-called **coupling terms** can only be analyzed visually by comparing the measured and theoretical transfer functions.
The main goal of this research is focussed on the bearing stiffness rather than bearing damping. However, the measured transfer functions yield both stiffness and damping values. Therefore, also the damping results are presented. In Lim's theory the damping is assumed to be Rayleigh damping, (proportional to the stiffness). The given radial damping results show that the damping decreases in case of an increasing preload; the Rayleigh damping appears not to be realistic. In [7] several damping models are discussed and also some experimental radial damping results are presented. These results also show a decrease in the radial damping for higher preloads. The results in [7] also show that the damping changes for a rotating shaft.

The same procedure has been applied to a specific angular contact bearing, since these bearings exhibit a greater contact angle, see Figure 6. Like for the deep groove ball bearing case, all modelled stiffnesses are smaller than the experimentally determined data. The stiffness trends however, are described well. The differences can be caused by the fact that the total system behaviour is measured and not only the bearing behaviour or by the difference between the static nature of the model and the dynamic nature of the measurements. Static bearing stiffness measurements can give clarification on this matter. Unlike in the deep groove ball bearing case, the measured angular contact damping values all decrease with increasing preloads. Apparently, the contact angle of a bearing influences the amount of damping.

5.2 Hysteresis and Reproducibility

Applying a higher axial preload and subsequently releasing the preload, shows the effect of hysteresis in a bearing. This is shown in Figure 7. Apparently, there is no hysteresis. The repeatedly performing of the

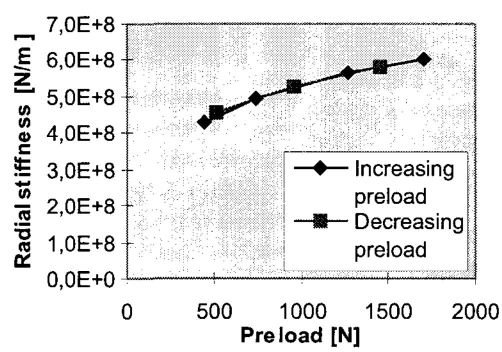

Figure 7: Measured radial stiffness, during increasing and decreasing preload. (Deep groove ball bearing NSK 6208)

measurements proved that the experimen-

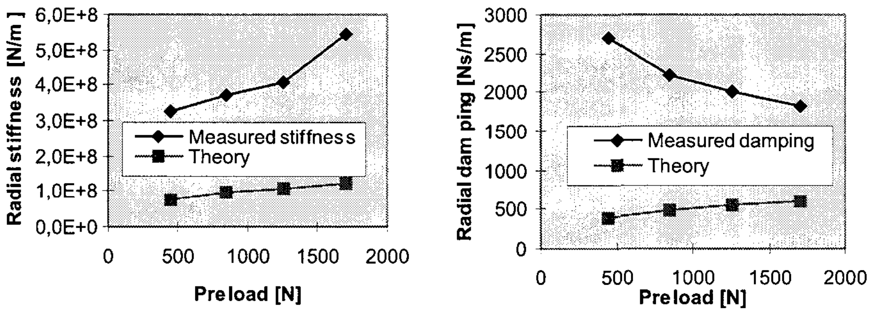

Figure 6: Left: The measured and theoretical *radial* stiffness. Right: The measured *radial* damping compared with the used Rayleigh damping. (Angular contact bearing RPF 7208)

tal setup is capable of producing the same results under the same circumstances later on. However, the hysteresis experiment stiffnesses, printed in Figure 8 together with the previous acquired radial stiffness results, are higher than the previously measured results. In the period between the hysteresis measurements and the actual stiffness measurements, a constant preload was applied on the bearing, which always kept the same position. From the figure the supposition can be drawn that the rolling elements are 'pulled through' the oil film or damaged under the high preload, especially because of the last experimental stiffness, which seems to be out of proportion. Performing the same measurements after creating a new oil film by rotating the shaft manually or putting the bearing in another position yielded the same stiffness values as obtained in the hysteresis experiment. Therefore, the influence of time has yet to be investigated.

5.3 Coupling Terms and Reciprocity

The theoretical model implicitly will always lead to a symmetric matrix. In Figure 9 the deep groove ball bearing transfer functions $H_{x\theta_y}$, $H_{\theta_y x}$, H_{yz}, H_{zy}, $H_{z\theta_x}$ and $H_{\theta_z z}$ are drawn. $H_{x\theta_y}$ and $H_{\theta_y x}$ show a great resemblance. The other terms however have less similarity, which could be explained by the fact that the actual radial preload, i.e. the weight of the shaft, is low.

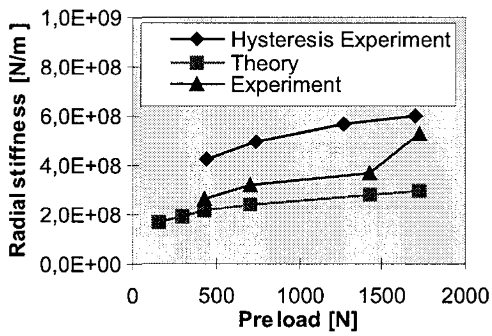

Figure 8: Hysteresis results compared with previous radial stiffness results

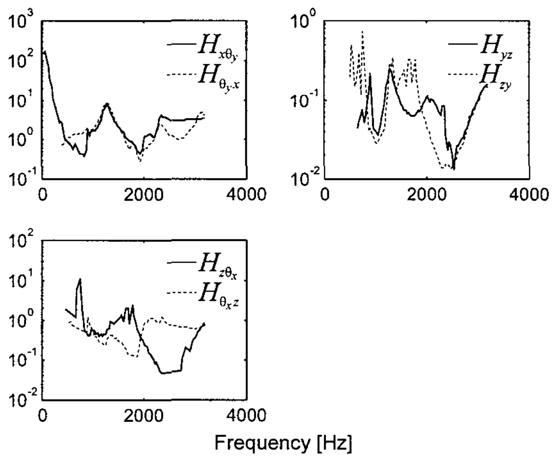

Figure 9: Verification of the transfer matrix symmetry. (Deep groove ball bearing NSK 6208, axial preload = 427 $[N]$)

6. Conclusions and Recommendations

6.1 Conclusions

• Reproducible measurements with acceptable coherence are possible (especially di-

rect FRF's). The stiffness results from the hysteresis experiment appeared to be higher than the actual stiffnesses, probably caused by the prolonged static preload.
• The concept of amplitude-weighting was not sufficiently effective to systematically reduce estimation errors.
• The direct estimation of the entire stiffness matrix appeared to be unfeasible.
• sdof fits on FRF-coupling terms can only be evaluated indirectly (graphically).
• Hysteresis in the bearing stiffness can be ignored.
• Experimental stiffnesses are higher than theoretical stiffnesses. However, the model is able to describe the stiffness trends.
• The radial bearing damping tends to decrease for increasing axial preload in the deep groove ball bearing case. In the angular contact bearing case **all** damping values decrease for increasing axial preload.
• The experiments seem to support the model's symmetry.

6.2 Recommendations

• Experiments with combined preloads have yet to be performed.
• For the mathematical model verification static experiments might clearify some existing discrepancies, but for more realistic data a rotating shaft should be applied.
• The effect long-term high preload cases without shaft rotation should be studied. This is probably related to the lubrication matter.
• Research on lubrication and damping matters are an obvious next step in this project.

References

[1] Lim, T.C. and Singh, R. (1990): *Vibration transmission through rolling element bearings in geared rotor systems*, NASA contractor report 4334, Ohio State University, Ohio, USA.

[2] Staps, E. (1995): *Identificatiemethodieken ter bepaling van de stijfheidsmatrix van wentellagers*, WFW rapport 95.077, Eindhoven University of Technology, Eindhoven, The Netherlands.

[3] Roosmalen, A.N.J. van (1994): *Design tools for low noise gear transmissions*, Ph.D. thesis, Faculty of Mechanical Engineering, Power Transmissions and Tribology Laboratory, Eindhoven University of Technology, Eindhoven, The Netherlands.

[4] Schroën, H.G.M. (1990): *Lager, Verwerking van een mathematisch lagermodel tot het computerprogramma Lager*, NOVEM-project "Geluidarme tandwieloverbrengingen", Eindhoven University of Technology, Eindhoven, The Netherlands.

[5] Rinawi, A.M. and Clough, R.W. (1991): *Improved amplitude fitting for frequency and damping estimation*, University of Berkeley, USA.

[6] Kraus, J.; Blech, J.J. and Braun, S.G. (1987): *In Situ determination of rolling bearing stiffness and damping by modal analysis*, Journal of Vibration, Acoustics, Stress and Reliability in Design **109**, 235-240, Faculty of Mechanical Engineering, Technion-Israel Institute of Technology, Haifa, Israel.

[7] Dietl, P.; Zeillinger, R.; Springer, H. (1996): *Experimentelle Identifikation und Berechnung des Dämpfungsvermögens von Kugellagern*, VDI Berichte **1285**, 259-273, Vienna, Austria.